Pressure-Induced Sublattice Disordering in SnO_2: Invasive Selective Percolation

Helainne T. Girao,[1] Patrick Hermet,[2] Bruno Masenelli,[3] Julien Haines,[2] Patrice Mélinon,[1] and Denis Machon[1,*]

[1]*Institut Lumière Matière, Université de Lyon, Université Claude Bernard Lyon 1, CNRS UMR 5306, 69622 Villeurbanne, France*
[2]*ICGM, CNRS, Université de Montpellier, ENSCM, UMR 5253, 34095 Montpellier CEDEX 5, France*
[3]*Institut des Nanotechnologies de Lyon INL CNRS-UMR5270, INSA-Lyon, 69622 Villeurbanne, France*
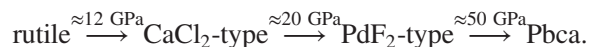
SnO_2 powders and single crystal have been studied under high pressure using Raman spectroscopy and *ab initio* simulations. The pressure-induced changes are shown to drastically depend on the form of the samples. The single crystal exhibits phase transitions as reported in the literature, whereas powder samples show a disordering of the oxygen sublattice in the first steps of compression. This behavior is proposed to be related to the defect density, an interpretation supported by *ab initio* simulations. The link between the defect density and an amorphouslike Raman signal is discussed in terms of the invasive percolation of the anionic sublattice. The resistance of the cationic sublattice to the disorder propagation is discussed in terms of cation close packing. This result on SnO_2 may be extended to other systems and questions a "traditional" crystallographic description based on polyhedra packing, as a decoupling between both sublattices is observed.

Metal dioxides MO_2, where M includes IVA and IVB cations such as Si, Ge, Sn, Pb, Ti, Zr, and Hf have received special attention because of their technological (ceramics) and geophysical interests. Their polymorphism is rich, and many studies have been dedicated to the understanding of their phase transitions under high pressure. Their structural transformations are usually described in terms of changes in the polyhedra packing. In addition to the usual polymorphic phase transitions, a transformation from a crystalline to an amorphous state has been observed in SiO_2 and GeO_2. This phenomenon has been intensively studied, and several parameters were found to play a role such as hydrostaticity and/or the form of the sample (powder vs single crystal) [1,2]. However, the underlying detailed mechanisms still remain to be elucidated. One of the means to unravel the structural mechanisms of this pressure-induced amorphization (PIA) effect has been to study isostructural or isochemical series of compounds such as berlinites (e.g., $AlPO_4$). Noticing that in SnO_2 such PIA has never been reported despite a consistent amount of work, we would like to adopt a different point of view in answering the following question: Why does SnO_2 not show PIA while Sn belongs to the same column of the periodic table as Si and Ge? Is this distinctive characteristic related to atomistic or structural reasons?

Under pressure, the sequence of phase transitions in bulk SnO_2 determined by x-ray diffraction techniques is [3,4]

$$\text{rutile} \xrightarrow{\approx 12 \text{ GPa}} \text{CaCl}_2\text{-type} \xrightarrow{\approx 20 \text{ GPa}} \text{PdF}_2\text{-type} \xrightarrow{\approx 50 \text{ GPa}} \text{Pbca}.$$

There is only one study dedicated to optical spectroscopies (Raman and Brillouin) of SnO_2 under pressure [5].

This work on a single crystal shows that, under pressure, the rutile-type phase ($P4_2/mnm$) transforms to a $CaCl_2$-type structure ($Pnnm$) at 14.8 GPa through a ferroelastic transition driven by the softening of the B_{1g} mode corresponding to a collective displacement of O atoms [4–6].

No sign of amorphization or disordering has been reported in these studies on bulk SnO_2. However, recently, a high-pressure study of SnO_2 nanoparticles using Raman spectroscopy has shown a pressure-induced disordering of the anionic sublattice. In fact, while x-ray diffraction, mainly sensitive to the cationic sublattice, does not show any transformation in a sample of 3 nm particles up to 30 GPa [7], Raman spectroscopy probing the oxygen sublattice demonstrates that some pressure-induced disordering occurs at around 14 GPa [8]. This study underlined the interest of combining experimental techniques to obtain a complete picture of the structural evolution. The rutile structure is particularly adapted to such decoupled studies of sublattices, as only the oxygen atoms are involved in the Raman-active vibrational modes [9].

The present work aims at exploring the pressure-induced phase transformation in a bulk SnO_2 crystal of various forms (powders and single crystal) by Raman spectroscopy, as it is a particularly interesting technique, mainly sensitive to the anionic sublattice, to complement the x-ray diffraction data on pressurized SnO_2. If previous high-pressure studies seem to give a coherent picture of the phase transition mechanism in a SnO_2 single crystal, we find here a more complex behavior in the case of powder samples. The observed differences will be discussed on the basis of the density of defects and interpreted in the framework of the percolation theory. The decoupling of

sublattices during pressure-induced transformations is an original framework to describe structural phase transitions.

High pressure was generated using a diamond-anvil cell with low-fluorescence diamonds. Samples were placed into a 125 μm chamber drilled in an indented stainless steel gasket. Depending on the experiments, no pressure-transmitting medium (PTM), 4:1 methanol:ethanol, or paraffin oil were used. The pressure was probed by the shift of the fluorescence line of a small ruby chip.

Raman spectra were obtained using a LabRAM HR Evolution spectrometer (Horiba Scientific) using an excitation energy of 532 nm and a power set at 5 mW to avoid heating. The beam was focused on the sample using a 50$\times$ objective, with a beam diameter $\sim$2 μm at the sample. The scattered light was collected in backscattering geometry using the same objective.

First-principles calculations are performed within the density functional theory framework as implemented in the ABINIT package [10]. The exchange-correlation energy functional is evaluated using the local density approximation parametrized by Perdew and Wang [11]. The all-electron potentials are replaced by norm-conserving pseudopotentials. Sn($4d^{10}, 5s^2, 5p^2$) and O($2s^2, 2p^4$) electrons are considered as valence states. The electronic wave functions are expanded in plane waves up to a kinetic energy cutoff of 60 Ha, and integrals over the Brillouin zone are approximated by sums over an $8 \times 8 \times 8$ mesh of special k points according to the Monkhorst-Pack scheme [12]. The dynamical matrix, dielectric constants, and Born effective charges are calculated within a variational approach to the density functional perturbation theory. Phonon dispersion curves are interpolated according to the scheme described by Gonze et al. [13]. The dipole-dipole interactions are subtracted from the dynamical matrices before the Fourier transformation, so that only the short-range part is handled in real space. We considered a $2 \times 2 \times 2$ q-point grid for the calculation of the phonon band structure, and a denser $100 \times 100 \times 100$ grid is used for the calculation of the phonon density of states.

Two different commercial powders were studied under high pressure: one from Aldrich (purity > 99.99%) and one from Merck (purity > 99.0%). X-ray diffraction shows that both samples are microcrystalline with an initial structure corresponding to the rutile type with no additional phase [14]. A third sample is a natural non-oriented single crystal (from Viloco mine, Bolivia). No x-ray diffraction experiment was performed on this sample; however, the Raman spectrum of the single crystal used for the high-pressure experiment is similar to those of the powders with three main peaks corresponding to the first-order spectrum (see Supplemental Material [14]) of the rutile structure.

SnO$_2$ adopts a tetragonal rutile structure. Each tin atom is at the center of six oxygen atoms located at the corners of a regular octahedron. The vibrational representation of
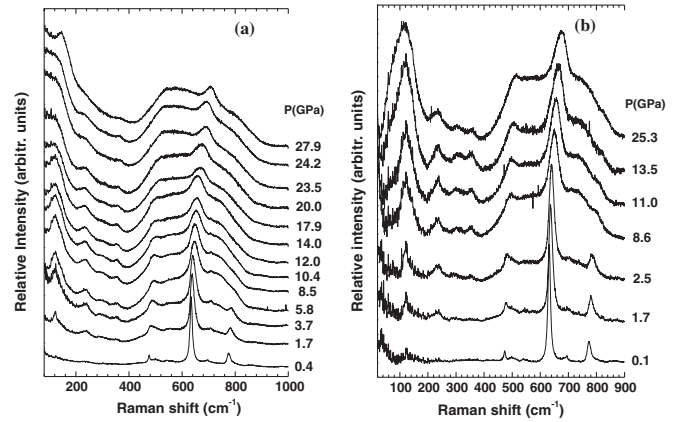

FIG. 1. (a) Raman spectra of SnO$_2$ powder (Aldrich) with increasing pressure (no pressure-transmitting medium). (b) Raman spectra of SnO$_2$ powder (Merck) with increasing pressure (no pressure-transmitting medium).

the normal modes at the center of the Brillouin zone is given by [9]

$$\Gamma = A_{1g}(R) + A_{2g} + B_{1g}(R) + B_{2g}(R) + E_g(R) \\ + A_{2u}(IR) + 2B_{1u} + 3E_u(IR).$$

In the four Raman-active modes (A_{1g}, B_{1g}, B_{2g}, and E_g), the oxygen atoms vibrate while Sn atoms are at rest. The positions of three peaks are well established with $\omega(E_g) \sim 475$ cm^{-1}, $\omega(A_{1g}) \sim 634$ cm^{-1}, and $\omega(B_{2g}) \sim 776$ cm^{-1} (Fig. 1). However, as the B_{1g} mode is a libration mode, it is difficult to observe and is absent in several spectra reported in the literature. Its position has been a matter of debate and has been reported as lying from 87 to 184 cm^{-1} (see [5,16,17], and references therein). Our simulation of the Raman spectra of rutile SnO$_2$ locates the peak position at $\sim$102 cm^{-1} with an intensity ratio $I(B_{1g})/I(A_{1g})$ equal to 5×10^{-5} [14], confirming the difficulty to observe this peak.

High-pressure experiments using Raman spectroscopy were carried out without a pressure-transmitting medium on both powder samples (Aldrich and Merck). The spectra are plotted in Figs. 1(a) and 1(b), respectively, and show a similar evolution.

In the first steps of compression, a background appears between 400 and 850 cm^{-1}. This change is concomitant with the growth of new peaks at lower frequencies ($\sim$122, $\sim$235, and $\sim$355 cm^{-1}). In particular, the low-frequency mode around 122 cm^{-1} rapidly increases in intensity and leads to a strong feature above 8.6 GPa. The Raman spectrum changes drastically at a low pressure, but further compression does not induce a strong additional qualitative change. The general shape of the spectra does not change with an increasing pressure even above $\sim$11 GPa, where one expects a phase transition to the CaCl$_2$-type structure

[4], although such a transition could be expected to occur at a lower pressure due to nonhydrostatic stress.

The appearance of broad bands is consistent with a disordering of the structure and may be attributed to a PIA. However, reports in the literature based on x-ray diffraction experiments do not support this conclusion, as such a transformation has never been observed. Nevertheless, Haines and Léger [4] noticed that, when a powder is compressed using a pressure-transmitting medium that does not ensure hydrostaticity (silicon grease), Rietveld refinements are no longer satisfactory at 5.0 GPa along with some broadening of the diffraction peaks and the diffraction patterns were correctly indexed using a $CaCl_2$ structural model but with a slightly larger cell parameter.

It is known that nonhydrostaticity can promote an amorphous state instead of the crystalline phase [1,2,18]. To check the effect of hydrostaticity, the same powder was loaded with a 4 : 1 methanol-ethanol mixture as the pressure-transmitting medium to ensure hydrostatic compression up to ~10 GPa [19]. Raman spectra show a general pressure-induced evolution roughly identical to the case without a pressure-transmitting medium [14]. The main difference lies in the relative intensity between the low-frequency and the high-frequency regions at a high pressure. The interplay between the morphology of the sample and the hydrostatic conditions during the compression are difficult to decouple. Thus, even compressing a powder sample with a PTM that provides good hydrostaticity may lead to an amorphouslike signature because of intergrain contact that induces local shear stresses [20]. Therefore, to investigate the effect of (i) the form of the sample and (ii) hydrostaticity, the following part is dedicated to the high-pressure study of a

SnO_2 single crystal immerged in paraffin oil (Fig. 2). Hydrostaticity is ensured up to around 3 GPa.

The Raman peaks upshift with an increasing pressure. Their pressure-induced evolutions are reported in Fig. 2(b), and values of the linear pressure dependence of the frequencies are reported in Ref. [14]. These results are in good agreement with the *ab initio* simulations [open symbols in Fig. 2(b)] and with the values reported in the literature [5]. In the present study, the B_{1g} mode is not measured. However, at a pressure around 7 GPa, a low-frequency peak is observed at ~75 cm^{-1}. With an increasing pressure, this peak upshifts but keeps a low intensity until 11.3 GPa, where it gains in intensity, becoming the most intense peak in the Raman spectra as expected in the $CaCl_2$-type structure. The change in the slope of $\nu(P)$ of other peaks is in agreement with the lowered transition pressure that may be due to the effect of nonhydrostatic stress components, as a coupling between the order parameter and strain has been demonstrated in the case of a similar ferroelastic transition in dense (stishovite) SiO_2 [21].

The main question at this point is the origin of such discrepancies between the high-pressure behaviors of powder and single-crystalline samples.

The broad features observed in powders during compression resemble a vibrational density of states (VDOS) observed when the Raman selection rules are broken because of the presence of disorder. The simulated VDOS of the rutile structure at 3.8 GPa has been computed and is compared with the experimental spectrum at the same pressure [Fig. 3(a)]. The observed bands in the Raman spectrum are in good agreement with the maxima of the phonon density of states. With increasing pressure and taking into account a structural transformation to the $CaCl_2$-type form, the experimental data are well reproduced by the simulations [Fig. 3(b)]. For instance, the peak at ~122 cm^{-1} is found to remain at the same position with
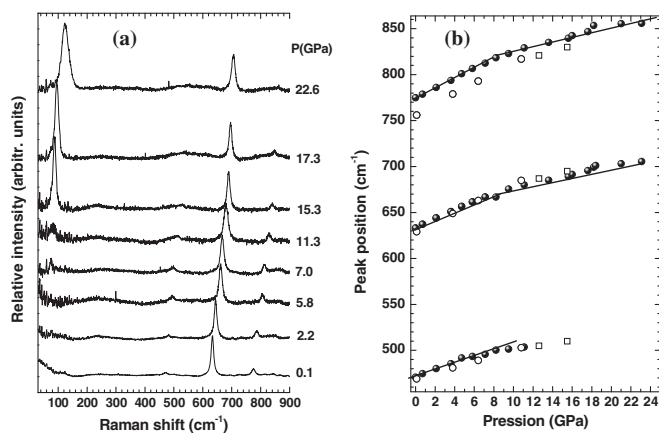

FIG. 2. (a) Selection of Raman spectra of an unoriented SnO_2 single crystal under pressure using paraffin oil as the pressure-transmitting medium. (b) Peak position as a function of pressure (closed circles, experimental; open circles, *ab initio* simulations for the rutile-type structure; open squares, *ab initio* simulations for the $CaCl_2$-type structure). The difference between experiments and simulations may be because, in *ab initio* calculations, the system is at $T = 0$ K.
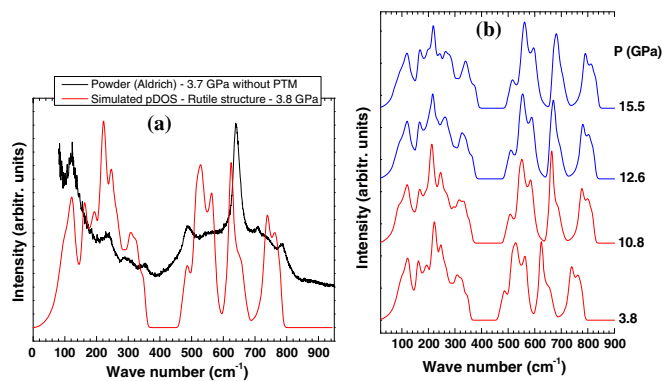

FIG. 3. (a) A comparison of the Raman spectrum of SnO_2 powder with a calculated phonon density of states of the rutile structure at ~3.8 GPa. (b) Simulated VDOS at different pressures in rutile (red lines) and $CaCl_2$-type (blue lines) structures. Phonon dispersion curves at 3.8 and 15.5 GPa are available as Supplemental Material [14].
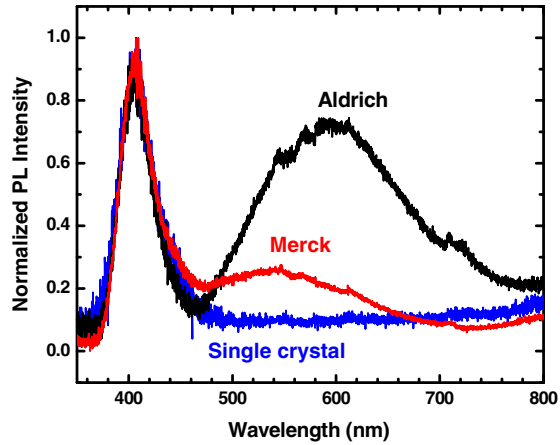
FIG. 4. Normalized photoluminescence spectra, excited at 266 nm, of the different SnO_2 samples. Aldrich and Merck correspond to two different powder samples.

increasing pressure in both simulations and experiment. It has to be noted that the B_{1g} mode has sometimes been reported at ~ 120 cm^{-1} at an ambient pressure [16,17]. This attribution of the B_{1g} mode should then be revised, and this peak should be assigned to a mode activated by the presence of defects.

In our case, it appears that the disordering affecting Raman spectra only implies the oxygen sublattice to which Raman spectroscopy is very sensitive to as in the case of pressure-induced transformations in nanoparticles [8]. To the best of our knowledge, such a decoupling between sublattices in simple, dense structures has never been reported [22]. In complex structures of rare earth molybdates, a two-step amorphization has been observed whatever the form of the samples. The anionic sublattice starts to exhibit amorphouslike Raman, photoluminescence, or EXAFS signatures at a lower pressure than the cationic sublattice probed by x-ray diffraction [23,24]. However, amorphization pressures for both sublattices are significantly lower in a powder than for a single crystal. Partial (sublattice) amorphization has also been discussed in $Co(OH)_2$, where infrared spectroscopy reported a disordering of the O-H sublattice. Interestingly, in $Ca(OH)_2$, a disordering of Ca-O and O-H sublattices occurred simultaneously [25].

To determine the origin of the disordering, Fig. 4 shows the photoluminescnece (PL) spectra of the different samples at ambient pressure. PL is an efficient technique to probe the defect density by reflecting the existence of defects, creating an electronic state in the band gap. According to several studies [26–29], several radiative desexitation paths are possible, all involving oxygen vacancies. Therefore, it is difficult to assign the peak positions in the photoluminescence spectra shown in Fig. 4, but it clearly appears that the single crystal shows a drastically lower radiative defect concentration and, thus, a lower defect concentration

compared to the powder samples (Aldrich and Merck) that contain mainly oxygen vacancies.

In summary, we observe a correlation between the defect density initially present in the samples and the selective disordering in SnO_2 upon compression. This correlation can be explained by invasive percolation as discussed in the following. Such an approach has been used with some success in the case of size-dependent pressure-induced amorphization by explaining the decrease of the pressure of amorphization with a decreasing nanoparticle size [30].

Long-range correlations are needed in a crystalline solid that undergoes a structural phase transition, as all sites must change their bonding or coordination state simultaneously to preserve the translational symmetry [31]. However, these long-range correlations can be affected by crystal defects: Atoms are statically displaced from an ideal lattice and can be viewed as perturbations to the lattice introducing local fluctuation. Defects can be present initially or created during the compression process, and a high defect density may in turn favor local correlations and the formation of local amorphous states.

A Voronoi cell can be defined around each defect. When approaching the stability field of the amorphous state, this cell can present two possible states: a crystal-like or an amorphouslike state. This is a percolating system where we can define the "experimental" crystal-to-amorphous transition at the percolation threshold. Percolating systems have a parameter q which controls the occupancy of sites (Voronoi cell) in the system. This parameter represents the probability for a site to be amorphous. The Voronoi cells are independent, but the number of amorphous cells grows with an increasing pressure and shear stresses developing in powder samples. This corresponds to an invasive percolating system where the amorphous state is the invader and can penetrate an isolated crystallized region (so-called defender). This is called invasive percolation without trapping. It has been established that percolation without trapping and regular percolation are of the same universality class [32]. Thus, a microscopic description of the transition at a local order is not necessary. The propagating disorder leads to an amorphouslike (VDOS) Raman spectra at the percolating threshold as discussed in Ref. [30].

This invasive percolation is restricted to the oxygen sublattice, and the cationic sublattice is resistant to this invasive percolation and local fluctuations. This property seems related to the closed packing of the cations. Indeed, in the rutile and $CaCl_2$-type structures, the Sn atoms are arranged through a centered tetragonal lattice. In the PdF_2-type form, this sublattice slightly evolves to a fcc arrangement. Therefore, the pressure-induced phase transitions mainly involve the oxygen sublattice [4]. The cationic sublattice that is close-packed-like may act as a rigid backbone, showing only pressure-induced distortion without diffusion. This strongly supports recent papers on oxides reporting the observation that the crystal structures

and even the unit cell dimensions of oxides depend on cation-cation interactions [33,34]. For instance, the Sn sublattice in the rutile-type structure, but also in tin oxide fluorides, adopts the atomic arrangement of the high-pressure allotrope γ-Sn [35]. The changes in the oxygen sublattice that are responsible for the phase transitions allow defects in this substructure to propagate. Our results support the "anions in metallic matrices" model, where a crystal structure of an inorganic compound may be described as a metallic matrix whose geometric and electronic structures govern the localization of the anions in the lattice [36].

Such an explanation of the resistance to PIA may be extended to other examples. In ZnO, no PIA has been reported. In the case of defective nanocrystals, Raman spectra resembling a VDOS appear at $P = 9$ GPa, the transition pressure from the wurtzite to the rocksalt structure. X-ray diffraction does not report such disordering, an observation similar to the case of bulk SnO_2. On the contrary, in ZnO nanoparticles with a very low defect concentration, no such VDOS has been observed using Raman spectroscopy [37]. A close inspection of the cationic sublattice indicates that Zn atoms in the wurtzite structure are arranged through an hcp packing. In the high-pressure rocksalt structure, cations are also in a fcc close-packed arrangements.

Generally, a crystallographic description of a structure relies on the packing of fundamental building blocks usually taken as a cation-centered polyhedron. For instance, we described rutile and $CaCl_2$-type structures as made of SnO_6 octahedra. This "traditional" picture implicitly assumes strong coupling between cationic and anionic sublattices, an idea that is questioned by our results where disordering occurs in a sublattice without implications for the cations. Such an idea has also been discussed in the case of quartz, where only the anion-anion interactions are found to be involved in the pressure-induced tetrahedral distortions [38]. However, nonclose packing of silicon atoms would lead to pressure-induced transformations in both sublattices. In addition, sublattice disordering in SnO_2 questions the effects of the defect density in the observation of PIA in SiO_2 and GeO_2. For instance, in SiO_2, depending on the sample form and on the hydrostaticity conditions, an amorphous state may be observed [1,2]. The transition to the stable high-pressure rutile-type form, stishovite, requires a major rearrangement of both cation and anion sublattices, giving rise to competition between the amorphous form and crystalline phases. An initial defect density may thus favor a disordering of the anionic sublattice that induces a destabilization of the quartz structure contrary to SnO_2, where the cationic sublattice remains ordered.

———————

[*] denis.machon@univ-lyon1.fr

[1] D. Machon, F. Meersman, M. C. Wilding, M. Wilson, and P. F. McMillan, Prog. Mater. Sci. 61, 216 (2014).

[2] P. Richet and P. Gillet, Eur. J. Mineral. 9, 907 (1997).

[3] S. R. Shieh, A. Kubo, T. S. Duffy, V. B. Prakapenka, and G. Shen, Phys. Rev. B 73, 014105 (2006).

[4] J. Haines and J. M. Léger, Phys. Rev. B 55, 11144 (1997).

[5] H. Hellwig, A. F. Goncharov, E. Gregoryanz, H.-K. Mao, and R. J. Hemley, Phys. Rev. B 67, 174110 (2003).

[6] S. D. Gupta, S. K. Gupta, P. K. Jha, and N. N. Ovsyuk, J. Raman Spectrosc. 44, 926 (2013).

[7] Y. He et al. Phys. Rev. B 72, 212102 (2005).

[8] H. T. Girão, T. Cornier, S. Daniele, R. Debord, M. A. Caravaca, R. A. Casali, P. Mélinon, and D. Machon, J. Phys. Chem. C 121, 15463 (2017).

[9] P. Merle, J. Pascual, J. Camassel, and H. Mathieu, Phys. Rev. B 21, 1617 (1980).

[10] X. Gonze et al., Comput. Phys. Commun. 180, 2582 (2009).

[11] J. P. Perdew and Y. Wang, Phys. Rev. B 45, 13244 (1992).

[12] H. J. Monkhorst and J. D. Pack, Phys. Rev. B 13, 5188 (1976).

[13] X. Gonze, J.-C. Charlier, D. C. Allan, and M. P. Teter, Phys. Rev. B 50, 13035 (1994).

[14] See Supplemental Material at http://link.aps.org/supplemental/10.1103/PhysRevLett.120.265702 for Raman spectra and x-ray diffraction patterns at ambient pressure; Results of Le Bail refinements on powder samples; Simulated Raman spectra of Rutile-type SnO_2; Raman spectra of compressed Merck sample using methanol:ethanol as the PTM; Pressure dependencies of the Raman peaks in the case of the single crystal; Comparison of Raman spectra at high pressure and after pressure cycle for all experiments; Phonon dispersion curves for rutile and $CaCl_2$-type structures, which includes Refs. [4,5] and [15].

[15] W. H. Baur and A. A. Khan, Acta Crystallogr. Sect. B 27, 2133 (1971).

[16] P. S. Peercy and B. Morosin, Phys. Rev. B 7, 2779 (1973).

[17] K. N. Yu, Y. Xiong, Y. Liu, and C. Xiong, Phys. Rev. B 55, 2666 (1997).

[18] P. Tolédano and D. Machon, Phys. Rev. B 71, 024210 (2005).

[19] R. J. Angel, M. Bujak, J. Zhao, G. D. Gatta, and S. D. Jacobsen, J. Appl. Crystallogr. 40, 26 (2007).

[20] D. Machon, V. P. Dmitriev, P. Bouvier, P. N. Timonin, V. B. Shirokov, and H. P. Weber, Phys. Rev. B 68, 144104 (2003).

[21] R. J. Hemley, J. Shu, M. A. Carpenter, J. Hu, H. K. Mao, and K. J. Kingma, Solid State Commun. 114, 527 (2000).

[22] For a discussion on the notion of complexity of a structure, see S. V. Krivovichev, Crystallography Reviews **23**, 2 (2017).

[23] O. Le Bacq, D. Machon, D. Testemale, and A. Pasturel, Phys. Rev. B **83**, 214101 (2011).

[24] D. Machon, V. P. Dmitriev, V. V. Sinitsyn, and G. Lucazeau, Phys. Rev. B **70**, 094117 (2004).

[25] J. H. Nguyen, M. B. Kruger, and R. Jeanloz, Phys. Rev. Lett. **78**, 1936 (1997).

[26] D. R. Miller, R. E. Williams, S. A. Akbar, P. A. Morris, and D. W. McComb, Sens. Actuators B **240**, 193 (2017).

[27] V. Bonu, A. Das, S. Amirthapandian, S. Dhara, and A. K. Tyagi, Phys. Chem. Chem. Phys. **17**, 9794 (2015).

[28] J. Jeong, S.-P. Choi, C. I. Chang, D. C. Shin, J. S. Park, B.-T Lee, Y.-J. Park, and H.-J. Song Solid State Commun. **127**, 595 (2003).

[29] J. X. Zhou, M. S. Zhang, J. M. Hong, and Z. Yin, Solid State Commun. **138**, 242 (2006).

[30] D. Machon and P. Mélinon, Phys. Chem. Chem. Phys. **17**, 903 (2015).

[31] N. D. Mermin and H. Wagner Phys. Rev. Lett. **17**, 1133 (1966).

[32] M. Porto, S. Havlin, S. Schwarzer, and A. Bunde Phys. Rev. Lett. **79**, 4060 (1997).

[33] A. Vegas and M. Jansen, Acta Crystallogr. Sect. B **58**, 38 (2002).

[34] A. Vegas and M. Mattesini, Acta Crystallogr. Sect. B **66**, 338 (2010).

[35] D. Santamaria-Pérez, A. Vegas, and U. Müller, Solid State Sci. **7**, 479 (2005).

[36] A. Vegas, D. Santamaria-Pérez, M. Marqués, M. Florez, V. Garcia Baonza, and J. Manuel Recio, Acta Crystallogr. Sect. B **62**, 220 (2006).

[37] D. Machon, L. Piot, D. Hapiuk, B. Masenelli, F. Demoisson, R. Piolet, M. Ariane, S. Mishra, S. Daniele, M. Hosni, N. Jouini, S. Farhat, and P. Mélinon, Nano Lett. **14**, 269 (2014).

[38] R. M. Thompson and R. T. Downs, Am. Mineral. **95**, 104 (2010).